



Modeling of SPAD avalanche breakdown probability and jitter tail with field lines

Rémi Helleboid, Denis Rideau, Jeremy Grebot, Isobel Nicholson, Norbert Moussy, Olivier Saxod, Jérôme Saint-Martin, Marco G. Pala, Philippe Dollfus

► To cite this version:

Rémi Helleboid, Denis Rideau, Jeremy Grebot, Isobel Nicholson, Norbert Moussy, et al.. Modeling of SPAD avalanche breakdown probability and jitter tail with field lines. Solid-State Electronics, 2022, 194, pp.108376. 10.1016/j.sse.2022.108376 . hal-03793952

HAL Id: hal-03793952

<https://cnrs.hal.science/hal-03793952>

Submitted on 18 Nov 2022

HAL is a multi-disciplinary open access archive for the deposit and dissemination of scientific research documents, whether they are published or not. The documents may come from teaching and research institutions in France or abroad, or from public or private research centers.

L'archive ouverte pluridisciplinaire **HAL**, est destinée au dépôt et à la diffusion de documents scientifiques de niveau recherche, publiés ou non, émanant des établissements d'enseignement et de recherche français ou étrangers, des laboratoires publics ou privés.

Modeling of SPAD avalanche breakdown probability and jitter tail with field lines

Rémi Helleboid^{a,b,c}, Denis Rideau^c, Jeremy Grebot^c, Isobel Nicholson^c,
Norbert Moussy^b, Olivier Saxod^b, Jérôme Saint-Martin^a, Marco Pala^a,
Philippe Dollfus^a

^a*Université Paris–Saclay, CNRS, Centre de Nanosciences et de Nanotechnologies,
Palaiseau, France*

^b*CEA LETI, Grenoble, France*

^c*STMicroelectronics, Crolles, France - Edinburgh, UK*

Abstract

A new methodology to accurately simulate the Photon Detection Efficiency and the Jitter tail of SPAD devices is presented. This method first relies on the use of the electric field lines to mimic the carriers' trajectories. A model for impact ionization and avalanche probability is then used on the obtained lines to simulate the probability of avalanche, coupled with the optical absorption, the PDE is then extracted. Finally, an advection-diffusion model is used to simulate the drift and diffusion of carriers within the device, which leads to the timing jitter due to the transport time from the photogeneration spot to the avalanche region. The results obtained numerically are compared with an extensive series of measurements and show a good agreement on a wide variety of device designs.

1. Introduction

Due to its high sensitivity, high photon detection efficiency (PDE), and high timing resolution, single-photon avalanche diodes (SPADs) have been widely used in a variety of applications during the last several decades. A micrometric silicon (Si) PN junction linked to neighboring CMOS devices and biased above

Email address: `remi.helleboid@st.com` (Rémi Helleboid)

the breakdown voltage is currently leading the market of SPADs. In the future development of SPADs, optimization of the PDE in the near infrared spectrum will be critical. This must be accomplished by designing the device layout and procedure without jeopardizing timing properties, particularly timing jitter.

As a result, it is critical to be able to test design improvements without having to wait for silicon production, which necessitates predictive modeling. The state-of-the-art in PDE and jitter prediction relies on computationally intensive Monte Carlo simulation [1, 2]. We present a substitute technique that combines the McIntyre model [3] with statistical jitter calculation along electric field lines.

The reference SPAD design used in this work is similar to the one presented in [4]. The junction is made of an N+ over P doping region. Additional low doping regions are created to prevent the SPAD from breaking laterally [5]. A graphic representation of the device is reported in 1

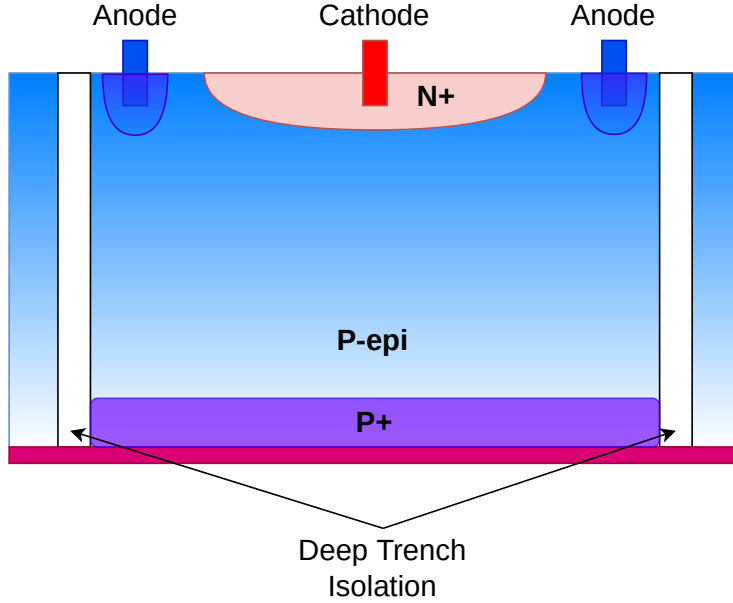


Figure 1: SPAD schematic architecture. Contacts are surrounded by high doping levels to create low Ohmic resistance. Each SPAD is isolated from the surrounding environment by deep trench isolation oxide layers to prevent optical and electrical cross-talk.

2. Model and simulation

The initial material of the presented simulation is the electrostatic simulation of the considered device architecture. This is obtained by performing process and electrical simulation of a numerically designed device layout, with, respectively, Sentaurus Process and Sentaurus Device program.

Both avalanche breakdown probability and jitter simulation then start with the computation of the electric field lines. The electric field lines are the lines that are everywhere parallel to the field vector. While these lines are usually used to visualize a vector field, in our case, they also represent the average path of carriers within the device. Indeed, if the stochastic effects in charge transport are overlooked, or averaged, the resultant trajectories are the electric field lines. To simulate the transport of an electron-hole pair photogenerated at a given position X_0 , the field line starting at X_0 is computing both forward (hole path) and backward (electron path). On each point of the field line, the electric field intensity and the doping concentration are interpolated from the process and device simulation, which let us with two sets of one dimensional data: the electric field, and the doping concentration along the field line.

The avalanche breakdown probability is then obtained by solving the McIntyre [3] model over many field lines. The McIntyre model, in its differential form, is a coupled, non-linear, boundary problem. Let $P_e(x)$ be the probability that a photogenerated electron starting at any point x in the device volume triggers an avalanche and $P_h(x)$ the same probability for a hole starting at x . The McIntyre problem hence reads:

$$\begin{cases} \frac{dP_e}{dx} = (1 - P_e)\alpha_e(P_e + P_h - P_eP_h) \\ \frac{dP_h}{dx} = -(1 - P_h)\alpha_h(P_e + P_h - P_eP_h) \end{cases} \quad (1)$$

$$\begin{cases} \frac{dP_e}{dx} = (1 - P_e)\alpha_e(P_e + P_h - P_eP_h) \\ \frac{dP_h}{dx} = -(1 - P_h)\alpha_h(P_e + P_h - P_eP_h) \end{cases} \quad (2)$$

with $0 \leq x \leq L$ where L is the total length of the carrier trajectory. α_e and α_h are the impact ionization coefficients, i.e. the number of impact ionization per unit distance, respectively for electrons and holes. Electrons are moving towards decreasing x (i.e. from right to left), and are collected at $x = 0$, thus the

probability for an electron to create an avalanche after being injected at $x = 0$ is zero. The same reasoning applies to holes at $x = L$. These considerations lead to the following boundary conditions:

$$\begin{cases} P_e(x = 0) = 0 \\ P_h(x = L) = 0 \end{cases} \quad (3)$$

It is solved by the means of an ad-hoc solver which uses finite-difference coupled with a Newton scheme embedded in a C++ solver [6]. The typical result of the model is shown over multiple field lines in Figure 2. By doing the computation from many starting points within the device, one is able to establish a map of avalanche breakdown probability which gives the probability that an avalanche will be triggered from an electron-hole pair generated at a given point. By multiplying this map by the local optical absorption (OA) map, and by integrating over the device's volume, one obtains the total Photon Detection Probability (PDP). The final PDE is then computed by scaling down the PDE by the optical fill factor (FF): $PDE = PDP * FF = BrP * OA * FF$.

By this technique, one can also detect bad device designs at simulation level. Indeed, if the doping profile and its associated process of fabrication is not carefully created, it can lead to electrostatic pockets or barriers. Those electrostatic defects will prevent photogenerated carriers to be transported from their generation location within the device's volume towards the avalanche region. Such a deficient device is shown in figure 3 with an applied voltage of 3V above the breakdown voltage.

In SPAD devices, jitter timing arises from two sources: the avalanche build-up timing and carriers' transport time from the photogeneration site to the avalanche region [7]. This study only focuses on the second source, indeed, the avalanche build-up occurs in typically tens of picoseconds, while transport timing can be up to several nanoseconds in SPAD with a large collection volume. The tail of the jitter is then almost only made by the carrier transit time within

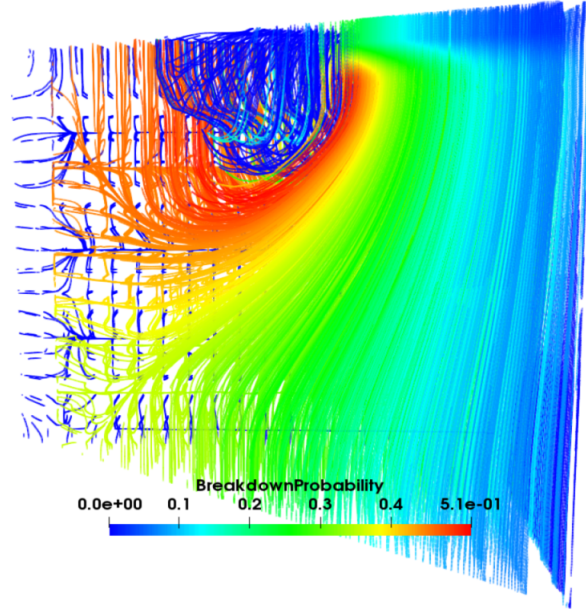


Figure 2: Breakdown Probability computed over multiple field lines. These field lines are computed along the electric field and mimic the individual carrier's trajectories from the departure at the point of photo-generation up to the junction. For accurate 3D calculation of breakdown probability, a great number of calculations is needed (typically 500 000). For the purpose of visualization only 8000 are shown in this figure.

the device. The diffusive transport is model by the advection-diffusion [8]:

$$\frac{\partial f}{\partial t}(x, t) = -\frac{\partial(u \cdot f)}{\partial x}(x, t) + \frac{\partial}{\partial x} \left(D \cdot \frac{\partial f}{\partial x} \right) (x, t) \quad (5)$$

Where D is the diffusion coefficient, u the carrier velocity and f the probability density function of carrier presence. By solving this equation along field lines, from many starting points, one can establish the histogram of transit times from generation location to the avalanche region.

Canali's model for velocity saturation at high field [9], together with Arora model for mobility in Silicon [10] were used to obtain the carrier velocity along the field lines. The diffusion is computed through the Einstein relation $D = \frac{\mu k_B T}{q}$.

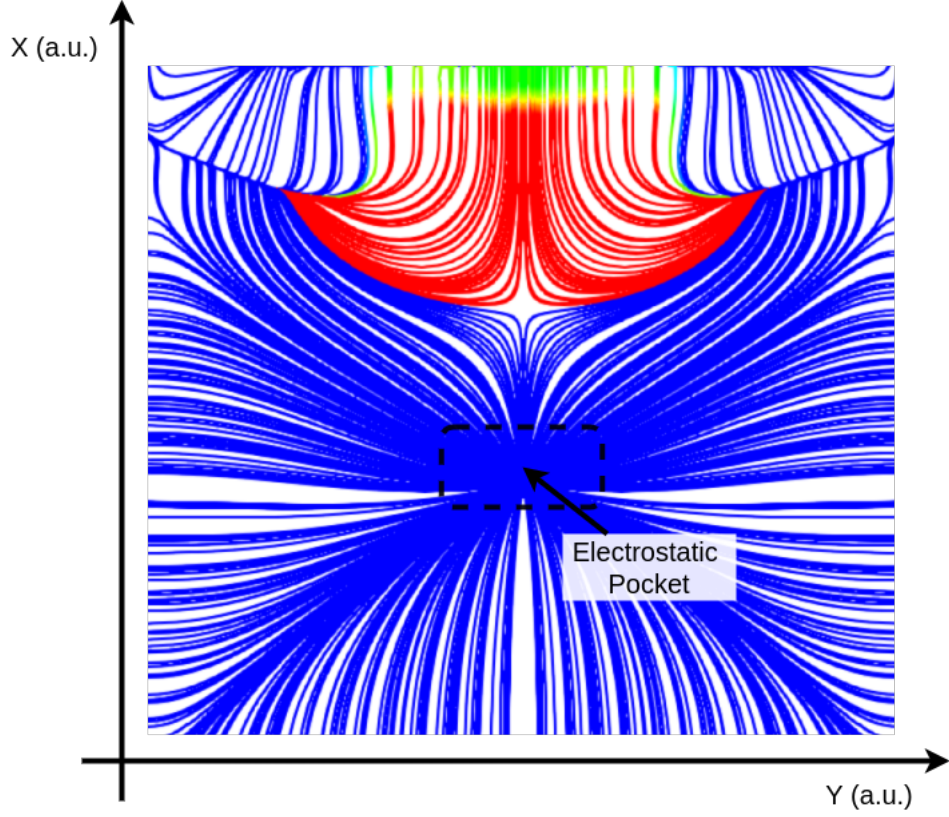


Figure 3: Ill-formed device. The electric field is focused on an electrostatic pocket in the center of the device. This prevents carriers from reaching the avalanche region and from triggering avalanches. The blue lines correspond to path with zero avalanche probability, while the red ones correspond to high avalanche breakdown probability.

3. Results and discussion

The simulations are validated by performing comparisons with experimental data on manufactured devices. The avalanche breakdown probability model can accurately predict the PDE, at different applied voltages, see Figure 4 The measured jitter tail also shows a good agreement with the simulation using advection-diffusion method, see Figure 5

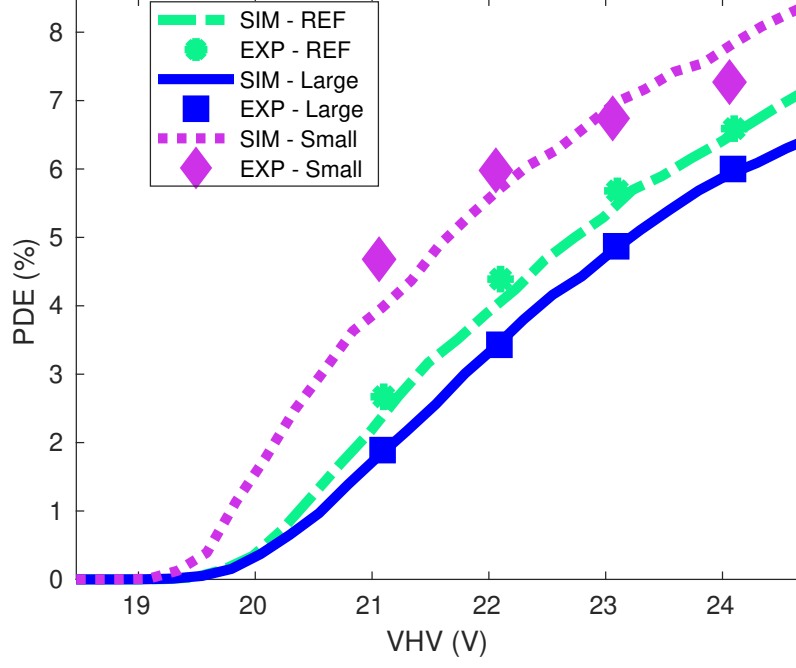


Figure 4: Comparison of PDE measured and simulated on three architecture variations.

4. Conclusion

Because advanced SPADs devices have extremely curved electric fields, one-dimensional avalanche breakdown probability models cannot be used. The one-dimensional McIntyre model is integrated over numerous field lines from several photogeneration starting locations within the device to solve this challenge. This enables accurate prediction of the local avalanche breakdown probability, which is then turned into photon detection efficiency by linking it with the device's optical simulation.

The jitter histogram's tail is predicted using the same idea. On the field lines, a one-dimensional drift-diffusion model is employed to simulate carrier drift-diffusive transit from their absorption location to the avalanche zone.

Both models are put to the test by comparing their results to those of produced SPADs.

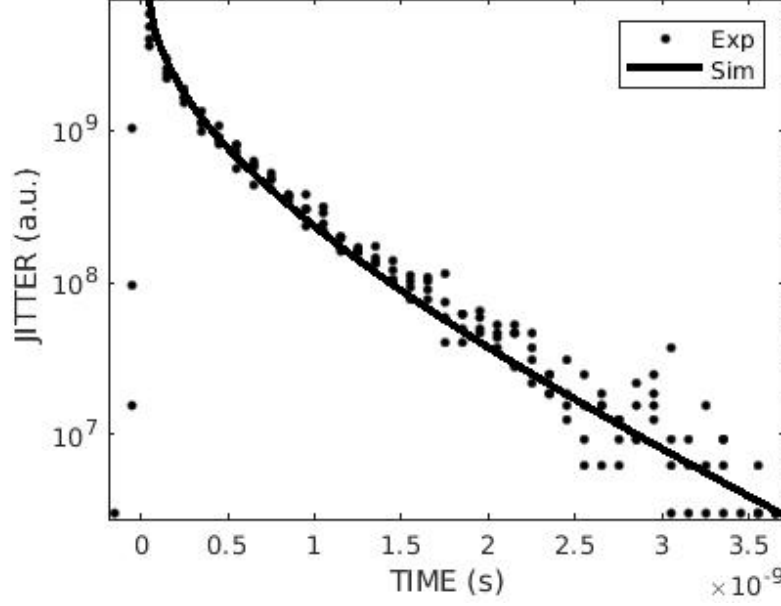


Figure 5: Comparison between characterization and simulation for jitter histogram.

The models may be utilized to properly predict PDE and jitter tail with simulations, as shown by the good agreement between simulation and characterization data.

Acknowledgment

This work was also supported by the French "Association Nationale Recherche Technologie" ANRT and the French GeSPAD Project of the Agence Nationale de la Recherche (ANR-20-CE24-0004).

References

- [1] D. Dolgos, H. Meier, A. Schenk, B. Witzigmann, Full-band Monte Carlo simulation of high-energy carrier transport in single photon avalanche diodes: Computation of breakdown probability, time to avalanche break-

- down, and jitter, *Journal of Applied Physics* 110 (2011) 084507–084507. doi:10.1063/1.3652844.
- [2] T. Cazimajou, M. Pala, J. Saint-Martin, R. Helleboid, J. Grebot, D. Rideau, P. Dollfus, Quenching Statistics of Silicon Single Photon Avalanche Diodes, *IEEE Journal of the Electron Devices Society* 9 (2021) 1098–1102. doi:10.1109/JEDS.2021.3127013.
- [3] R. McIntyre, A new look at impact ionization-Part I: A theory of gain, noise, breakdown probability, and frequency response, *IEEE Transactions on Electron Devices* 46 (8) (1999) 1623–1631. doi:10.1109/16.777150.
- [4] R. Helleboid, D. Rideau, I. Nicholson, N. Moussy, O. Saxod, M. Basset, J. Grebot, A. Zimmerman, B. Mamdy, D. Golanski, M. Agnew, S. Pellegrini, M. Sicre, Comprehensive modeling and characterization of photon detection efficiency and jitter in advanced spad devices, in: *ESSDERC 2021 - IEEE 51st European Solid-State Device Research Conference (ESSDERC)*, 2021, pp. 271–274. doi:10.1109/ESSDERC53440.2021.9631801.
- [5] W. Wang, Y. Zhang, Z. Wei, High-Performance Structure of Guard Ring in Avalanche Diode for Single Photon Detection, *International Journal of Communications, Network and System Sciences* 10 (8) (2017) 1–6. doi:10.4236/ijcns.2017.108B001.
- [6] U. M. Ascher, R. M. M. Mattheij, R. D. Russell, *Numerical Solution of Boundary Value Problems for Ordinary Differential Equations*, 1st Edition, Society for Industrial and Applied Mathematics, Philadelphia, 1987, pp. 194–205.
- [7] A. Spinelli, A. L. Lacaita, Physics and numerical simulation of single photon avalanche diodes, *IEEE Transactions on Electron Devices* 44 (11) (1997) 1931–1943. doi:10.1109/16.641363.
- [8] C. Jacoboni, P. Lugli, *The Monte Carlo Method for Semiconductor*

Device Simulation, Springer-Verlag, 1989, pp. 72-74. doi:10.1007/978-3-7091-6963-6.

- [9] C. Canali, G. Majni, R. Minder, G. Ottaviani, Electron and hole drift velocity measurements in silicon and their empirical relation to electric field and temperature, IEEE Transactions on Electron Devices 22 (11) (1975) 1045–1047. doi:10.1109/T-ED.1975.18267.
- [10] N. Arora, J. Hauser, D. Roulston, Electron and hole mobilities in silicon as a function of concentration and temperature, IEEE Transactions on Electron Devices 29 (2) (1982) 292–295. doi:10.1109/T-ED.1982.20698.